International Journal of Heat and Mass Transfer 71 (2014) 217–227

Contents lists available at ScienceDirect

International Journal of Heat and Mass Transfer

journal homepage: www.elsevier.com/locate/ijhmt

Transient thermal boundary layers over rough surfaces

J.B.R. Loureiro [a,b,*], A.P. Silva Freire [a]

[a] Mechanical Engineering Program (PEM/COPPE/UFRJ), C.P. 68503, 21941-972 Rio de Janeiro, Brazil
[b] Mechanical Engineering Department (DEM/Poli/UFRJ), C.P. 68503, 21941-972 Rio de Janeiro, Brazil

ARTICLE INFO

Article history:
Received 29 July 2013
Received in revised form 26 November 2013
Accepted 26 November 2013
Available online 5 January 2014

Keywords:
Thermal boundary layer
Transient
Roughness
Error in origin
Reynolds analogy

ABSTRACT

The transient heat transfer convection in a turbulent boundary layer is theoretically and experimentally studied when a time-periodical step-wise heat flux is imposed upon a rough surface. In particular, the behavior of the displacement height for the thermal boundary layer and the validity of the Reynolds analogy are analyzed. The local boundary layer characteristics, friction velocity, friction temperature and the displacement heights for the velocity and the temperature profiles, are evaluated through the graphical method of Perry and Joubert (1963) [3]. The results indicate that the displacement heights assume very different values and that the Reynolds analogy hypothesis is satisfied.

1. Introduction

The flows that are encountered in nature and technology are essentially transient. In real conditions, no flow is truly subject to isothermal or constant heat flux wall conditions. The literature is permeated by studies in which spatial variations are analyzed, but temporal variations are often overlooked.

The increase in heat transfer rate provoked by the exposition of a turbulent flow to a rough wall is known to be considerably less than the corresponding increase in skin-friction. The matter is clearly discussed in Owen and Thomson [1]. As a simple argument, the transport of heat in the vicinity of a wall is controlled solely by a molecular property of the fluid, its thermal conductivity, whereas the shear stress is observed to depend on the form drag of individual protuberances. In other words, the pressure mechanism for the transfer of momentum finds no counterpart for the transfer of heat in flows over rough surfaces. The different transfer mechanisms for momentum and heat imply that characteristic parameters for the velocity and temperature profiles must behave distinctly, including the roughness effective length and the error in origin. For this reason, the Reynolds analogy between transfer processes must be modified to consider the local influence of the Reynolds and Prandtl numbers. These aspects are all discussed here.

The present work carries out an experimental study of the characteristics of a thermal turbulent boundary layer subject to transient heating on a rough surface. The purpose is to discuss the behavior of the unsteady Stanton number in varying wall temperature conditions as well as some other important parameters including the temperature error in origin, the enthalpy thickness and the thermal Clauser shape factor of the boundary layer. The work also develops an approximate analytical solution for the description of the unsteady temperature profile in the fully turbulent region of the boundary layer. The errors in origin for the velocity and temperature profiles are further discussed. In particular, it is shown that the physical interpretation for the velocity error in origin presented by Jackson [2] is not consistent.

The work shows that the classical methods of analysis can be used to find the changing properties of the unsteady temperature boundary layer, provided the necessary modifications are made.

Only forced convective heat transfer effects are considered here, that is, thermal boundary layers without coupling of the velocity and temperature fields. The work studies the response of the internal surface layer to a time-periodic, step-wise, heat flux imposed at the wall. Under these conditions, the friction velocity remains constant. The friction temperature, on the other hand, changes with time (as does the Stanton number). Indeed, in the experimental simulations, the wind tunnel is kept at a constant speed, so that the velocity field keeps its statistical properties unchanged. Thus, at any station for any given time, the wall shear stress has a constant mean value. However, the heat flux at the wall changes with time, as do the wall and friction temperatures.

The heat flux at the wall is evaluated from the mean temperature gradient in the fully turbulent logarithmic region of the flow.

* Corresponding author at: Mechanical Engineering Program (PEM/COPPE/UFRJ), C.P. 68503, 21941-972 Rio de Janeiro, Brazil. Tel.: +55 2136223548; fax: +55 2136223552.

E-mail addresses: jbrloureiro@gmail.com (J.B.R. Loureiro), atilafreire@gmail.com (A.P. Silva Freire).

0017-9310/$ - see front matter © 2013 Elsevier Ltd. All rights reserved.
http://dx.doi.org/10.1016/j.ijheatmasstransfer.2013.11.076

Nomenclature

A	parameter in velocity law of the wall
B	parameter in temperature law of the wall
C	parameter in transient temperature solution
C_i	parameter in roughness function
C_f	friction coefficient (=$2(u_\tau/U_\infty)^2$)
c_p	specific heat
d	displacement height (=$K-\varepsilon$)
D	parameter in transient temperature solution
E	parameter in transient temperature solution
F	solution of heat equation
g	gravity acceleration
G	Clauser parameter
G	solution of heat equation
G_h	defect enthalpy profile shape factor
H	height for estimation of R_i (=35 mm)
I	parameter in transient temperature solution
J	parameter in transient temperature solution
K_s	sand roughness length
K	height of protuberances
k	thermal conductivity
$\overline{K}$	average height of protuberances (=KS/λ)
l	mixing length
M	torque exerted by the horizontal stress on the top of the roughness elements
M_T	(=$\lambda d_T Q_0$)
M	parameter in transient temperature solution
N	parameter in transient temperature solution
P_r	Prandtl number
P_{r_t}	turbulent Prandtl number
p	pressure
Q	heat flux
Q	parameter in transient temperature solution
q	heat flux per unit area
R	parameter in transient temperature solution
R_e	Reynolds number
R_i	Richardson number (=$(gH/T)((T_H-T_w)/U_H^2)$)
S	width of protuberances
S	parameter in transient temperature solution
S_t	Stanton number (=$Q_w/(\rho c_p U_\infty(T_w-T_\infty))$)
t	time
t'	temperature fluctuation
T	temperature
T_{ij}	stress tensor
t_τ	friction temperature (=$Q_w/(\rho c_p u_\tau)$)
U, u	longitudinal velocity component
u_τ	friction velocity $\left(=\sqrt{\tau_w/\rho}\right)$
Δu	roughness function
x, z	flow Cartesian coordinates
w	transversal velocity component

Greek symbols

δ	velocity boundary layer thickness
δ_T	temperature boundary layer thickness
δ_i	height of control volume (Fig. 1)
δ_1	displacement thickness
δ_2	momentum thickness
Δ_h	enthalpy thickness
ϵ	small parameter (=$\sigma/(\varkappa_T u_\tau)$)
ε	error in origin
$\varkappa$	von Karman's constant (=0.4)
$\varkappa_T$	von Karman's constant for the temperature profile (=0.44)
λ	pitch of protuberances
μ	dynamic viscosity
ν_t	momentum eddy diffusivity
α_t	thermal eddy diffusivity
ρ	density
σ	separation variable (decaying rate of friction temperature)
τ	shear stress

Subscripts

0	quantity acting on the displacement plane
T	temperature
H	height where the Richardson number was evaluated
∞	external flow condition
w	wall condition

Superscripts

$'$	fluctuating quantity
$-$	mean quantity

In the graphical method of Perry and Joubert [3] and Perry et al. [4], the error in origin for the temperature profile, ε_T, is determined by adding arbitrary values to the wall distance measured from the top of the roughness elements. The value of ε_T that furnishes the best discriminated logarithmic region is then considered to be the correct value for the error in origin. Having found ε_T, one then can make use of the gradient of the log-law to determine the friction temperature. With the friction temperature, the friction velocity (taken from the mean velocity profile), the temperature at the wall and the properties of the fluid, the wall heat flux can then be evaluated.

As observed by Kalinin and Dreitser [5], "the problem of unsteady heat transfer is a conjugate one since the mathematical model for the description of heat transfer and hydrodynamics of a coolant is augmented with the equations of heat conduction in the material and with the conjugation conditions at boundaries". In the present work, as said before, the heat transfer rate is determined through a local analysis of the fully turbulent flow region.

In the next section, Section 2, a short review on turbulent heat transfer from rough surfaces is presented. The concept of the error in origin for the velocity and temperature boundary layer profiles is discussed in Section 3; an analytical solution for the unsteady temperature boundary layer in the fully turbulent region is also developed in Section 3. In the first part of Section 4, the experiments of Perry et al. [4], Loureiro et al. [6] and Antonia and Luxton [7] are used to discuss the concepts introduced in the paper of Jackson [2]. The second part describes the unsteady thermal boundary layer experiments and presents results for the varying friction temperature, enthalpy thickness, thermal Clauser shape factor of the boundary layer and Stanton number. Section 5 presents the final remarks.

2. Short literature review

Two key concepts for the interpretation of velocity and temperature data of turbulent boundary layers over rough walls are the roughness length and the error in origin (also known as the displacement in height or the zero-plane displacement). While a clear distinction is made in the literature regarding the behavior of the roughness lengths for the velocity and temperature fields (see, e.g., the works of Malhi [8] and Sun [9]), the position of the error in origin (ε) for both fields is normally considered identical or even not considered in the investigations. In the following short text, we illustrate how the error in origin concept is faintly discussed in analyses of the temperature profile. In fact, Raupach [10] argues that the error in origin is normally considered property independent for the pragmatic reason that independent assessments of ε and ε_T are not available.

The error in origin for the velocity profile was possibly first introduced by Einstein and El-Samni [11]. Using a Pitot tube, these authors managed to determine the wall shear stress by placing the theoretical wall some distance below a plane tangent to the top of the roughness elements. This approach was systemized by Perry and Joubert [3] and Perry et al. [4], who reviewed many rough-wall boundary layer experiments to propose a method to locate the vertical displacement of the origin below the crest of the roughness elements, the error in origin, ε. The resulting graphical method has been used ever since to determine the local boundary layer characteristics from measured mean velocity distribution.

In fact, even after the contribution of Einstein and El-Samni [11] and of other authors, the error in origin concept eluded some now classical work. Many early works studied the modification in boundary layer properties due to spatial changes in wall features. Despite the known limitations of wind tunnel experiments, valuable information on the response of turbulence to roughness changes in local advection was provided by Antonia and Luxton [7,12] and by Mulhearn [13], who resorted to the error in origin concept. On the other hand, previous authors had already formulated theories to describe a boundary layer passing through a step change in surface roughness. The theories of Elliott [14] and of Panofsky and Townsend [15] assumed that changes in velocity are self-preserving. Essentially, they considered that the streamwise changes in flow properties can be described by changes in the characteristic scales of velocity and roughness length. That approach, particularly, allows for a logarithmic distribution of velocity in the internal layer of the flow. In two following papers, Townsend [16,17] proposed better approximated solutions by considering the velocity and the temperature distributions to adjust to asymptotic solutions valid for very large values of $\log(l_0/z_0)$, where l_0 denotes the depth of the modified flow and z_0 the surface roughness length. The formulation of Townsend was revisited by Chan [18], whose theory, with the inclusion of higher-order terms, shows that much larger values of shear stress are possible in the flow downstream of a change in surface roughness. In these works, the theories are most simplified, self-preservation is assumed and the displacement height is not considered.

According to Jackson [2], the error in origin of the logarithmic velocity profile is a concept that is commonly surrounded by "a great deal of confusion". The objective of Jackson's paper was to discuss the physical interpretation of the displacement in height, showing that it could be regarded as the level at which the mean drag on the surface appears to act. In the developments, the displacement height was considered to be identical to the displacement thickness for the shear stress.

Loureiro et al. [6] discussed the distribution of wall shear stress downstream of a change in surface, from rough to smooth. The work shows that in regions where roughness alternate, the logarithmic region does not immediately settles to the local conditions. For this reason, wall shear stress calculations based on the slope of semi-logarithmic plots – and therefore on the displacement height – are rendered invalid.

Some of the first studies on the transfer of heat across rough surfaces were conducted in pipe flow and measured bulk quantities were in steady state conditions. Typical examples are the works of Owen and Thomson [1], Dipprey and Sabersky [19] and Han et al. [20]. These works resort to the "principle of Reynolds number similarity" and the "law of the wall similarity" to propose simple algebraic expressions for the rate of heat transfer in terms of the roughness Reynolds number and the Prandtl number.

The behavior of thermal boundary layers developing over surfaces with non-uniform heat flux or temperature distributions has been investigated by some authors in the past (see, e.g., [21–24]). Most of the studies, however, were concerned with flows over smooth surfaces. Coleman et al. [25] and Ligrani and Moffat [26] were the first to consider flows over rough surfaces. In both works, the authors used a kernel function to describe the Stanton number distributions. Coleman et al. [25] investigated flows subject to many varying boundary conditions: wall temperature, wall blowing, free-stream velocity, steps in wall temperature and steps in blowing. Ligrani and Moffat [26] concentrated on studying the effects of unheated starting lengths on the properties of flows that developed over a rough surface. No particular consideration was given to the velocity and temperature error in origin in the logarithmic profiles. Results were described in terms of the equivalent sand grain roughness.

An extension of the concept of error in origin to the temperature boundary layer was advanced by Avelino and Silva Freire [27] for surfaces of types 'K' and 'D' (see the classification of Perry et al. [4]).[1] The aim of the research was to investigate the behavior of the temperature error in origin when velocity and temperature boundary layers with different states of development were considered. Under these conditions, it was not clear that a straight Reynolds analogy would work for the calculation of the friction coefficient and of the Stanton number. For a positive answer, the values for the error in origin for the velocity and the temperature fields would have to have the same order of magnitude. In the experiments, a cold flow over a smooth surface was made to pass over a heated, rough surface. As it turned out, surfaces of type 'K' presented velocity and temperature errors in origin that seemed compatible whereas surfaces of type 'D' presented errors in origin with very different values.

Belnap et al. [28] have proposed a new Reynolds analogy based on measurements obtained in a rectangular cross-section channel with rough walls. Data analysis was based on global properties and resulted in an expression that differs from the expressions previously presented by Owen and Thomson [1], Dipprey and Sabersky [19] and Kays and Crawford [29].

3. Theory

3.1. The error in origin from first principles

Dimensional analysis plays a crucial role in modeling turbulent flow over rough walls for its inherent capacity to encapsulate all roughness geometric (and possibly stochastic) complexity in terms of few parameters such as the roughness length and the error in origin. The difficulty with this approach, of course, is that some of the physics may be missed due to a lack of formal derivation based on the first principles. Despite its known value, dimensional analysis assembles quantities taking into account just their dimen-

[1] Briefly: On a 'K' type roughness, eddies with a length scale proportional to the roughness height are assumed to be shed into the flow above the crests of the protuberances. The effects of roughness on the flow can be expressed with the help of a single length scale K and depend on Reynolds number. On a 'D' type roughness, the protuberances are closely spaced and stable vortices are trapped in the grooves. Eddy shedding from the protuberances into the flow is small. The friction coefficient is insensitive to the characteristic scale K, but depends on some other global scale of the flow.

sional coherence, without taking any notice to their physical interplay. A possible undesired outcome is that selected dimensionless groups may result in simple curve fittings, devoid of any physical meaning or interpretation.

Regarding the error in origin concept, a lack of a formal understanding of its physical meaning has led to some disagreement concerning its nature and how to correctly determine its value. This problem is further complicated by the fact that two parameters must be specified: the displacement heights for velocity and temperature, which are frequently used interchangeably in the literature, albeit they stand for different flux densities from the wall [8].

Here, ε for both velocity and temperature, is studied from arguments based on the first principles, the Navier–Stokes equation and the first law of thermodynamics. The developments of Jackson [2] are followed to derive an expression for ε (=$K - d$) in terms of the pressure distribution around a roughness element. An extension to the thermal case is obtained by an application of the same type of arguments to the first law of thermodynamics. Predictions are compared with results obtained from the gradient of the log-law. The experimental data of Perry et al. [4], Loureiro et al. [6] and Antonia and Luxton [7] show that both notions do not coincide.

3.1.1. The error in origin for the velocity profile

The error in origin was thought by Jackson [2] to be the level at which the mean drag, τ_0, on the surface appears to act.

Consider the control volume and the coordinate system shown in Fig. 1. Consider also that the flow variables are the same at sections AB and CD.

The x-momentum and continuity equations can be written as

$$\rho\partial_x\overline{u}^2 + \rho\partial_z\overline{u}\,\overline{w} = -\partial_x p + \partial_x T_{11} + \partial_z T_{12}, \tag{1}$$

$$\partial_x\overline{u} + \partial_z\overline{w} = 0, \tag{2}$$

with

$$T_{ij} = \mu\partial_j\overline{u_i} - \rho\overline{u_i'u_j'}. \tag{3}$$

The integration of Eq. (1) in x over the control volume, followed by a multiplication in z and a further integration in z, results in (see the full details in Jackson [2])

$$M = SK\tau_0 + \int_{fluid}(\tau_0 - (T_{12} - \rho\overline{u}\,\overline{w}))dxdz, \tag{4}$$

with

$$M = \int_0^K z\Delta p dz + K\int_0^S T_{12}dx. \tag{5}$$

Quantity Δp is the pressure difference between the lateral faces of the roughness elements; τ_0 denotes the average force per unity area acting on the displacement plane. The second integral in Eq. (5) represents the torque exerted by the horizontal stress on the

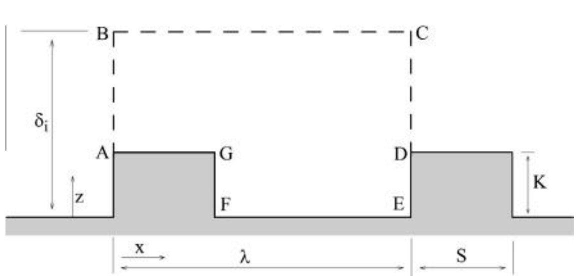

Fig. 1. Control volume over rough surface.

top of the roughness elements. The total moment acting on the roughness elements is thus given by M. This must equal the moment acting at the face BC, which can be written as $M_{BC} = \lambda d\tau_0$.

The result is

$$d - \overline{K} = (\lambda\tau_0)^{-1}\int_{fluid}(\tau_0 - (T_{12} - \rho\overline{u}\,\overline{w}))dxdz, \tag{6}$$

where, $\overline{K} = KS/\lambda$ is the average elevation of the surface.

Parameter d is interpreted by Jackson [2] as the level at which the mean drag on the wall appears to act. It can be related to the error in origin through the simple geometric relation $\varepsilon = K - d$.

Eq. (6) provides a full-blown expression for d (and for that matter for ε) which must be experimentally validated. To do this, consider the pressure drag to be the dominant effect in Eq. (5). It follows immediately that

$$M \approx \int_0^K z\Delta p dz, \tag{7}$$

so that

$$d \approx \frac{\int_0^K z\Delta p dz}{\int_0^K \Delta p dz}. \tag{8}$$

3.1.2. The error in origin for the temperature profile

The error in origin for temperature profile can be seen as the effective position of a heat source inside the roughness sublayer which imparts the heat flux in the logarithmic layer. To find a length scale associated to the heat flux, we follow the same procedure developed for the velocity field. This new length scale, d_T (=$K - \varepsilon_T$), is the analogous of the velocity displacement height d.

The heat transfer equation is cast as

$$\rho c_p(\overline{u}\partial_x\overline{T} + \overline{w}\partial_z\overline{T}) = \partial_x Q_x + \partial_z Q_z, \tag{9}$$

where

$$Q_i = k\partial_i\overline{T} - \rho c_p\overline{u_i't'}. \tag{10}$$

Eq. (9) is integrated over the control volume in x, followed by a multiplication in z and a further integration in z. The result is

$$\int_0^K z[-k\partial_x\overline{T}]_S^\lambda dz + K\int_0^K k\partial_z\overline{T}dx + \int_{fluid}(Q_z - \rho c_p\overline{w}\,\overline{T})dxdz$$
$$= \delta_i\int_0^\lambda[Q_z - \rho c_p\overline{w}\,\overline{T}]^{\delta_i}dx. \tag{11}$$

The first term on the lhs of the above equation represent the molecular heat flux difference between the roughness elements. The second term on the lhs is the molecular heat flux through the top of the elements. The last term on the lhs is proportional to the heat flux through the fluid in the control volume. The rhs represents the heat flux through the top face of the control volume. There is no net contribution coming from the lateral faces AB and CD since the flow variables are the same at both faces. Also, there is no contribution coming from the bottom surface between the elements since in Eq. (11) the heat flux is multiplied by a height, which vanishes at $z = 0$.

Eq. (11) can be re-written as

$$M_T = KSQ_0 + \int_{fluid}(Q_0 - (Q_z - \rho c_p\overline{w}\overline{T}))dxdz, \tag{12}$$

where Q_0 is the heat flux at the displacement plane and $M_T = \lambda d_T Q_0$.

The displacement in height for the temperature field becomes then

$$d_T - \overline{K} = (\lambda Q_0)^{-1}\int_{fluid}(Q_0 - (Q_z - \rho c_p\overline{w}\overline{T}))dxdz. \tag{13}$$

Eq. (13) can be simplified to

$$d_T = \frac{\int_0^K z[-k\partial_x \overline{T}]_S^{\lambda} dz + K\int_0^K k\partial_z \overline{T} dx}{\int_0^K [-k\partial_x \overline{T}]_S^{\lambda} dz + \int_0^K k\partial_z \overline{T} dx}. \quad (14)$$

Parameter d_T depends only on the molecular heat flux coming from the roughness elements. Thus, it is clear that both d and d_T depend on different physical parameters, and hence are unrelated quantities.

3.2. Steady state problem

Consider the problem of a given incompressible fluid flowing over a smooth, heated surface under a steady state condition [30]. The governing equations are Eqs. (1), (2) and (9). These equations must be solved under appropriate boundary conditions at the wall. For the velocity field, the no-slip condition and the permeability condition can be used. For the temperature field, a number of different possible boundary conditions can be specified. Basically, one can prescribe the wall temperature, the wall heat flux or a combination of these two.

Consider next that the turbulent boundary layer has a three-layered structure [31,32] and that, furthermore, in one of the existing layers the turbulence effects dominate.

Thus, in this layer, the governing equations reduce to:

x-Momentum:

$$\partial_z \overline{u'w'} = 0. \quad (15)$$

Heat transfer:

$$\partial_z \overline{w't'} = 0. \quad (16)$$

So that the above equations can be solved, a relation has to be established between the mean and the turbulent quantities. The simplest way of doing this is to invoke the concepts of eddy diffusivities for momentum and heat, together with the mixing-length hypothesis [30]. This results in the following algebraic equations for the turbulent quantities

$$-\partial_z \overline{u'w'} = \partial_z[\nu_t \partial_z \overline{u}] = \partial_z\left[l^2(\partial_z \overline{u})^2\right] = 0, \quad (17)$$

$$-\partial_z \overline{w't'} = \partial_z[\alpha_t \partial_z \overline{u}] = \partial_z\left[(l\partial_z \overline{u})(l_T \partial_z \overline{T})\right] = 0, \quad (18)$$

where ν_t and α_t denote the eddy diffusivities for momentum and heat.

We further incorporate into our analysis two extra hypotheses [30]:

1. von Karman's hypothesis that the mixing–length can be considered proportional to the wall distance, i.e. $l = \varkappa z$ and $l_T = \varkappa_T z$, where $\varkappa$ and $\varkappa_T$ are constants.
2. Prandtl's hypothesis that in the near wall region the total shear stress and the heat flux are constant.

Thus, upon a simple integration, it results that in the fully turbulent region the local solutions are given by:

$$\overline{u} = \frac{u_\tau}{\varkappa} \ln z + A, \quad (19)$$

and

$$T_w - T = \frac{t_\tau}{\varkappa_T} \ln z + B, \quad (20)$$

where $u_\tau = \sqrt{(\tau_w/\rho)}$, $t_\tau = Q_w/(\rho c_p u_\tau)$ and $\varkappa$ = 0.4.

The implication of Eqs. (19) and (20) is that, provided $\varkappa$ and $\varkappa_T$ are known, the skin-friction coefficient and the heat-transfer coefficient can be evaluated respectively from the slope of semi-log plots of distance from the wall versus velocity and distance from the wall versus temperature.

If a turbulent Prandtl number is defined [30], it follows that

$$Pr_t = \frac{\nu_t}{\alpha_t} = \frac{\varkappa}{\varkappa_T}. \quad (21)$$

A common sense in literature is that Pr_t varies across the boundary layer in a way that depends on both the molecular properties of the fluid and the flow field. In the logarithmic region, however, many authors (see, e.g., Simpson et al. [33], Blackwell et al. [34] and Chen [35]) have shown that Pr_t is approximately constant, resulting in a value of 0.44 for $\varkappa_T$.

3.3. Transient convection in turbulent boundary layers over smooth, flat surfaces

Consider now the problem of a given incompressible fluid flowing steadily over a surface with a prescribed heat flux.

Under this condition, the velocity field remains unaltered so that the velocity local solution in the fully turbulent region can still be approximated by the logarithmic equation, Eq. (19).

The thermal problem, however, suffers an important modification since the surface boundary conditions have to change to accommodate a time varying imposed heat flux.

Thus, it results that the energy governing equation reduces to

$$\partial_t T = -\partial_z \overline{w't'}. \quad (22)$$

The above equation can be re-written as

$$\partial_t T = \partial_z(u_\tau \varkappa_T z \partial_z T). \quad (23)$$

To find a solution, consider

$$T(z,t) = F(t)G(z). \quad (24)$$

Then upon substitution of Eq. (24) onto Eq. (23) it follows that

$$\frac{F'(t)}{F(t)} = u_\tau \varkappa_T \left[\frac{G'(z) + zG''(z)}{G(z)}\right]. \quad (25)$$

So that a solution is sought from equations

$$\frac{F'(t)}{F(t)} = -\sigma, \quad (26)$$

$$G'(z) + zG''(z) + \frac{\sigma}{u_\tau \varkappa_T} G(z) = 0, \quad (27)$$

where the sign of σ was chosen so as to ensure that the temperature will decay in time.

The solution of Eq. (26) is

$$F(t) = Je^{-\sigma t}. \quad (28)$$

To solve Eq. (27) consider the decaying time to be long enough so that $\epsilon = (\sigma/(\varkappa_T u_\tau))$ can be considered a small parameter. Then, search for a solution of the form

$$G(z) = G_0(z) + \epsilon G_1(z). \quad (29)$$

The substitution of Eq. (29) onto Eq. (27) and the collection of the terms of the same order yields

$$G_0'(z) + zG_0''(z) = 0, \quad (30)$$

$$G_1'(z) + zG_1''(z) + G_0(z) = 0, \quad (31)$$

whose solutions are

$$G_0(z) = C\ln z + D, \quad (32)$$

$$G_1(z) = E\ln z + Rz\ln z + Sz + Q, \quad (33)$$

with $R = C$ and $2C + D - S = 0$.

Thus, the fully turbulent approximate solution is given by

$$T(z,t) = Je^{-\sigma t}[(C\ln z + D) + (\sigma/(\varkappa_T u_\tau))(E\ln z + Rz\ln z + Sz + Q)], \tag{34}$$

where all constants must be determined experimentally.

3.4. Transient convection in turbulent boundary layers over rough, flat surfaces

If all above results are to be extended to flows over rough surfaces of the types 'K' or 'D', the classical three–layered structure of the boundary layer needs to be abandoned.

We know that for flows over 'K' or 'D' rough surfaces the viscous region is completely destroyed by the protuberances at the wall. Under this condition, the fully turbulent region just described above has to suffer some adjustments so as to yield a good description of the velocity and the temperature fields. Other authors [3,4,7,11] have shown that a universal expression can be written for the wall region provided the origin for measuring the velocity profile is set at some distance below the crest of the roughness elements, the error in origin, ε.

Thus, for any kind of rough surface, it is possible to write

$$\frac{\overline{u}}{u_\tau} = \frac{1}{\varkappa}\ln\left[\frac{(z_T+\varepsilon)u_\tau}{\nu}\right] + A - \frac{\Delta u}{u_\tau}, \tag{35}$$

where,

$$\frac{\Delta u}{u_\tau} = \frac{1}{\varkappa}\ln\left[\frac{\varepsilon u_\tau}{\nu}\right] + C_i; \tag{36}$$

the subscript T is used to indicate that the origin of the measured velocity profile is to be taken at the top of the protuberances (and this must not be confused with the subscript T used also to indicate temperature), $\varkappa = 0.4$, $A = 5.0$, and $C_i, i = K, D$; is a parameter characteristic of the roughness.

Eqs. (35) and (36), although of a universal character, have the inconvenience of needing two unknown parameters for their definition, the skin–friction velocity, u_τ, and the error in origin, ε. A chief concern of many works on the subject is, hence, to characterize these two parameters.

For an experimentalist, however, these equations are very useful for they provide a graphical method for the determination of the skin-friction coefficient.

To extend Eq. (34) to turbulent flows over rough surfaces we will draw a direct analogy with Eq. (35).

For flows over rough surfaces, we have seen that the characteristic length scale for the near wall region must be the displacement in origin. In this situation, the viscosity becomes irrelevant for the determination of the inner wall scale because the stress is transmitted by pressure forces in the wakes formed by the tops of the roughness elements. It is also clear that, if the roughness elements penetrate well into the fully turbulent region, then the displaced origin for both the velocity and temperature profiles will always be located in the overlap fully turbulent region.

The similarity in transfer processes for turbulent flows then suggests that

$$T(z,t) = Je^{-\sigma t}[(C\ln z^+ + D) + (\sigma/(\varkappa_T u_\tau))(E\ln z^+ + Rz^+\ln z^+ + Sz^+ + Q)], \tag{37}$$

where $z^+ = (z_T + \varepsilon_T)$ and the parameters to be determined may now be a function of the roughness.

In principle, the error in origin for the temperature, ε_T, should be time dependent.

Eq. (37), however, provides a good means to measure the heat flux at the wall. Provided we can evaluate the error in origin through one of the classical techniques, the slope of the temperature profile plotted in a semi-log graph will furnish the friction temperature and, thus, the heat transfer coefficient.

4. Experiments and discussions on parameterization

4.1. Error in origin

Jackson [2] postulated that the d's in Eqs. (8) and (35) (where $\varepsilon = K - d$) are the same. This hypothesis is here tested through the experimental data of Perry et al. [4], Loureiro et al. [6] and Antonia and Luxton [7]. In these works, individual roughness elements were fitted with pressure taps so as to permit the form drag method to be used to determine the wall shear stress. Of course, the same pressure difference profiles can be used to find ε. The result is shown in Table 1.

Antonia and Luxton [7] estimated just one value of d (=0.36$K = K - \varepsilon$) – through the log-law – that was assumed to hold at all stations. This estimated value (=1.14 mm) is much lower than those estimated through the form drag (=1.37 and 1.67 mm). The results of Loureiro et al. [6], on the other hand, show the opposite trend d_{loglaw} (=4.3 mm) > $d_{formdrag}$ (=2.5 mm). Both these works studied surfaces that are of type 'K'.

An analysis of the data of Perry et al. [4] for surfaces of type 'D' discloses d_{loglaw} (=25.02) > $d_{formdrag}$ (=22.67 mm).

Despite the large number of articles on rough surfaces available in literature, not many were identified by the present authors as admissible to put to test the postulate of Jackson concerning the physical meaning of d (or ε). Based on the results shown in Table 1, it appears that $d_{formdrag}$ and d_{loglaw} are uncorrelated quantities.

A DNS study conducted by Castro and Leonardi [36] shows that log-law fits obtained with independently known values of d (evaluated through Eq. (6)) and the wall shear stress can only be good provided $\varkappa$ is permitted to change. A tacit assumption in [36] is that "Jackson provided a convincing physical definition of d ...". In fact, as shown in Section 3, a parameter "d" can be defined through Eq. (6). However, the developments of [2] did not in any way show this "d" to be the same "d" defined through Eq. (35) (=$K - \varepsilon$). To do that, one should show that Eq. (6) substituted into Eq. (35) is a solution to Eq. (1) (fitted with any adequate turbulence model) or, more simply, to Eq. (15) (in case asymptotic arguments are summoned to show that in the fully turbulent region the approximated solution is governed by Eq. (15)). The instantaneous velocity profiles presented in [36], to show that both d's are the same, would have to produce an averaged profile that under an adequate processing would furnish a "d" compatible with Eq. (35). This "d" should then be compared with the one evaluated through the definition provided by Eq. (6).

The very detailed work on the estimation of surface characteristics by Cheng et al. [37] also supports the notion that both d's are not the same by quoting: "The results did not support the argument put forward in the literature that the zero-plane displacement could be reliably predicted from the height of the centre of drag force".

Table 1
Experimental comparison between $d_{formdrag}$ and d_{loglaw}. Dimensions are in mm.

Work	d (Eq. 8)	d (Eq. 35)
Perry et al. [4]	22.67	25.02
Antonia and Luxton [7]	1.37	1.14
Antonia and Luxton [7]	1.67	1.14
Loureiro et al. [6]	2.47	4.30

Eq. (14) could not be tested due to the absolute lack of experimental data. It has been shown here, however, to emphasize the arguments of Owen and Thomson [1] that the increase in heat transfer rate is controlled exclusively by the molecular properties of the fluid. Therefore, the error in origin for the velocity and temperature profiles cannot be the same quantity. This is shown in the next Section.

4.2. Stanton number

The unsteady heat transfer experiments are described next.

The principal facility used in the experiments was the large thermal wind tunnel of the Laboratory of Turbulence Mechanics of the Mechanical Engineering Program of COPPE/UFRJ. The studies were conducted as follows. For over 10,000 s a constant heat flux was applied to the test section. After this time, and for an extra 10,000 s, the heat was turned off. This cycle was repeated at least twice for every wind tunnel run. During the whole experiment, the flow velocity was kept constant; that assured a steady state condition for the velocity profile. The thermal boundary layer, however, was always in a transient state.

The laboratory was air conditioned and the temperature was maintained to within ±0.5 °C of the working temperature, 20 °C. The basic flow instrumentation consisted of thermo-anemometers and thermocouples.

A general view of the wind tunnel is shown in Fig. 2. The test section has an overall length of 10 m, and a cross section area of 0.67 m × 0.67 m. The external flow velocity can be made to vary from zero to 3.5 ms^{-1} with free stream turbulence intensity levels of about 2%. In still air conditions, the floor temperature can be raised up to 100 °C over a 6 m long surface. The heating system is comprised by a series of 6 one-meter independent panels fitted with electrical resistances that may furnish a wall temperature controlled variation of 2°C. The total heating capacity of each panel is about 0.75 kW m^{-2}. The whole facility is capable of developing boundary layer gradients of up to 60 °C at uniform mean speeds in the range of 1.5–3.5 ms^{-1}.

In all experiments, measurements of stream-wise velocity and temperature were made through thermo-anemometers and thermocouples. The velocity measurements were made with DANTEC anemometers of the series 56 M. The boundary layer probe was a DANTEC 55P15 model. Reference measurements for the velocity were obtained from a Pitot tube connected to an inclined manometer. The reference mean temperature profiles were obtained from chromel-constantan micro-thermocouples. The probe supports for both the velocity and the temperature probes were mounted on an automatic traverse gear system whose resolution is 0.02 mm.

An uncertainty analysis of the data was performed according to the procedure described in Kline [38]. Typically the uncertainty associated to the velocity and the temperature measurements were: U = 0.04 ms^{-1} precision, 0 bias (P = 0.95); T = 0.2 °C precision, 0 bias (P = 0.99).

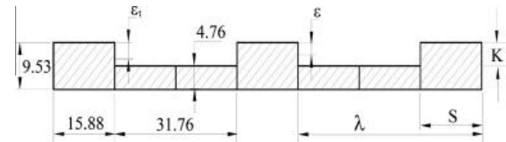

Fig. 3. Geometry of roughness protuberances. Dimensions are in millimeters.

The rough surface was constructed with equally spaced transversal rectangular aluminum bars. The dimensions of the roughness elements are shown in Fig. 3 where K denotes the height, S the width and λ the pitch of the protuberances.

To validate the equations presented in Sections 3 and 4, measurements were taken at one particular station, at 6500 mm downstream of the settling chamber (see Fig. 2).

At the testing station, the flow properties were those shown in Table 2 where δ_1 denotes the boundary layer displacement thickness, δ_2 the boundary layer momentum thickness and G the Clauser parameter (Eq. 38). This table incorporates the friction-velocity, a parameter whose determination will be explained next. The inflow air temperature was kept at 20 °C. The uncertainty associated to each variable is also shown in Table 2.

$$G = \Delta_2/\Delta_1 = \frac{\int_0^\delta ((U_\infty - u)/u_\tau)^2 dz}{\int_0^\delta ((U_\infty - u)/u_\tau) dz}. \tag{38}$$

The Clauser parameter, G, indicates the similarity state of the outer region of a turbulent boundary layer. Flows where G is independent of x are called "equilibrium flows" and can be expressed in terms of universal velocity-defect coordinates. A value of about G = 6.5 is normally accepted as implying equilibrium condition for flows over smooth walls.

The mean velocity profiles and the longitudinal turbulent intensity are shown in Figs. 4 and 5, respectively.

To determine the velocity error in origin, ε, the method of Perry and Joubert [3] was used. Thus, velocity profiles were plotted in semi-log graphs in dimensional coordinates. Initially, the normal distance from the top of the roughness elements was incremented by 0.1 mm and a straight line fit was applied to the resulting points. The best fit was chosen by searching for the maximum coefficient of determination, R-squared. Other statistical parameters were also observed, the residual sum of squares and the residual mean square. Normally, a coefficient of determination superior to 0.99 was obtained.

The determination of ε (=1.2 mm) is illustrated in Fig. 6.

Having found ε, we can then use the gradient of the log-law to determine u_τ. Another method to obtain u_τ is the momentum integral equation. This latter method, however, is very sensitive to any

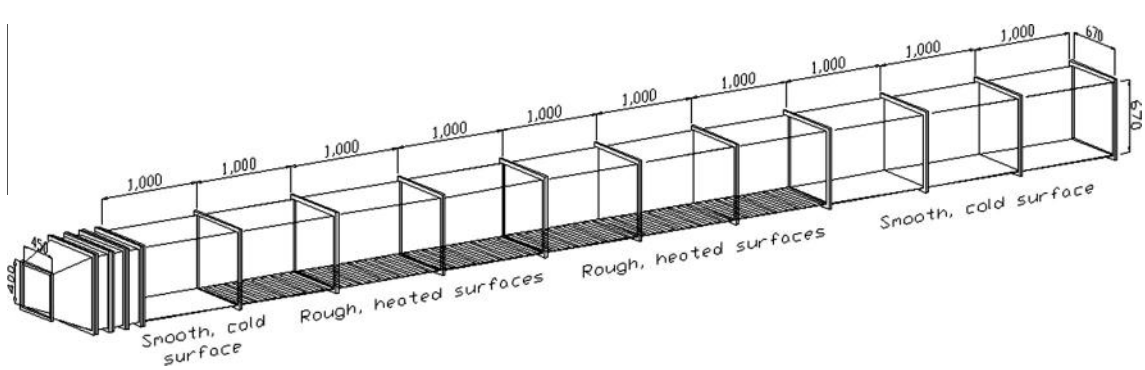

Fig. 2. General view of the wind tunnel.

Table 2
Experimental conditions.

Surface	U_∞ [ms^{-1}]	u_τ[ms^{-1}]	δ_1 [mm]
Smooth	3.0 ± 0.04	0.128 ± 0.04	13.22 ± 1.0
Rough	3.0 ± 0.04	0.161 ± 0.04	29.76 ± 1.0
	δ_2[mm]	G	q_w [kWm^{-2}]
Smooth	9.58 ± 1.0	6.61 ± 0.3	0.75 ± 0.7
Rough	18.74 ± 1.0	6.89 ± 0.3	0.75 ± 0.7

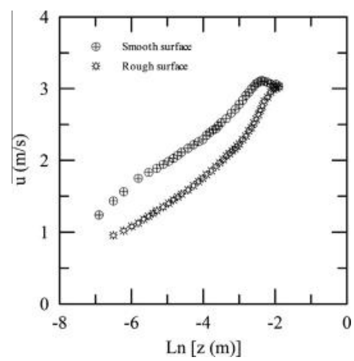

Fig. 4. Mean velocity profiles. Smooth and rough surfaces.

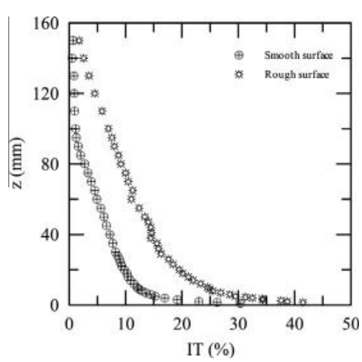

Fig. 5. Longitudinal turbulence intensity profiles. Smooth and rough surfaces.

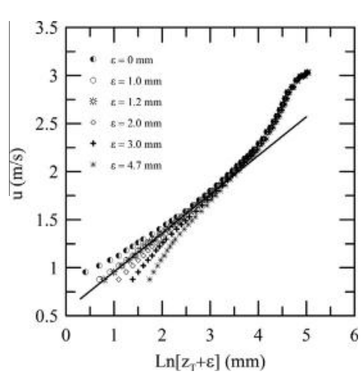

Fig. 6. Determination of ε according to the method of Perry and Joubert [3]. Curves were drawn for values of $\varepsilon = 0, 1, 1.2, 2, 3$ and 4.7 mm. Resulting $u_\tau = 0.161$ ms^{-1}.

three-dimensionality of the flow and the determination of the derivatives of the various mean flow parameters is a highly inaccurate process.

To record the temperature profiles, a special probe support was constructed. The probe held seven thermocouples separated vertically in fixed locations. Once the logarithmic region had been identified from the velocity measurements the seven thermocouples were positioned to characterize the thermal fully turbulent region.

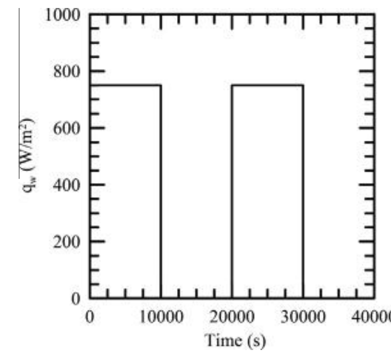

Fig. 7. Time history of wall heat flux.

The time history of the heat flux that was applied to the wall is shown in Fig. 7. Due to the large thermal inertia of the experimental set up resulting from the aluminum bars that defined the rough surface, the wall heat flux needed to be applied over a large time interval (10,000 s) to let the temperature profile reach an asymptotic steady state. Measurements were performed in the second cycle, when reproducibility conditions were observed. The resulting temperature time evolution in the boundary layer is shown in Fig. 8a (smooth surface) and Fig. 8b (rough surface). Characterization of the temperature evolution was very important for the determination of the friction temperature and the Stanton number. In particular, the shapes of the curves suggest that Eq. (37) exhibits the correct function behavior for data reduction.

The enthalpy thickness of the boundary layer is shown in Fig. 9. In the early part of the heating cycle, the higher near wall turbulence provoked by the roughness induces a faster development of the thermal boundary layer. Indeed, for time <10,000 s, the relation $(\Delta_h)_{rough} > (\Delta_h)_{smooth}$ is observed. In the cooling cycle, $10{,}000 < \text{time} < 20{,}000$ s, this trend is reversed. The higher rough wall turbulence induces a faster return to isothermal conditions, so that $(\Delta_h)_{rough} < (\Delta_h)_{smooth}$.

The state of development of the thermal boundary layer can be expressed in terms of the defect enthalpy profile shape factor, defined as

$$G_h = \Delta_4/\Delta_3 = \frac{\int_0^{\delta_T} ((T_\infty - T)/t_\tau)^2 dz}{\int_0^{\delta_T} ((T_\infty - T)/t_\tau) dz}. \tag{39}$$

In regions where G_h is constant, outer layer similarity is indicated. Fig. 10 shows that over most of the heating and cooling cycles, G_h is nearly constant, for both the smooth and rough surfaces.

The error in origin for the temperature profile, ε_T, was also determined through the method of Perry and Joubert [3]. Thus, the gradient of the temperature log-law was used to find the friction temperature, and, consequently, the local wall heat flux.

In the present experiment, temperatures up to 65°C were obtained at the wall. To estimate the effects of buoyancy forces and flow stability in the logarithmic region, we used the bulk Richardson number, defined by,

$$R_i = \frac{gH}{T} \frac{(T_H - T_w)}{U_H^2}, \tag{40}$$

where the subscripts H and w denote respectively quantities to be evaluated at height H (=35 mm) and at the wall; T denotes the average temperature.

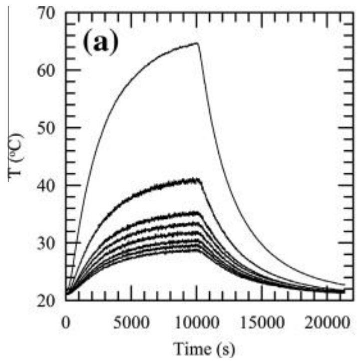

Fig. 8. Temperature evolution in the turbulent boundary layer: (a) smooth surface; curves from top to bottom: $z = 0, 1, 6, 11, 16, 23, 30, 36$ mm; z denotes wall distance. (b) Rough surface; curves from top to bottom: $z_T = -4.77, 1, 6, 11, 16, 23, 30, 36$ mm. z_T denotes distance from top of roughness elements.

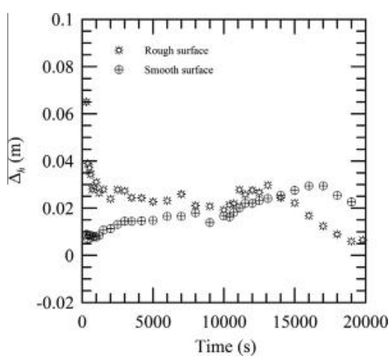

Fig. 9. Time history of Δ_h for the smooth and rough walls.

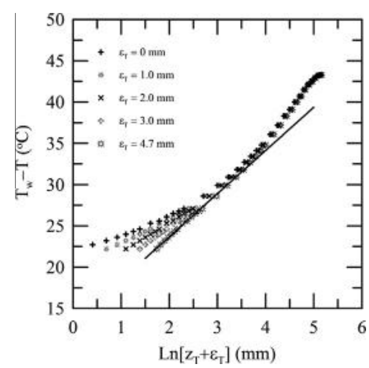

Fig. 11. Determination of ε_T according to the method of Perry and Joubert [3]. Curves were drawn for values of $\varepsilon_T = 0, 1, 2, 3$ and 4.7 mm. Resulting $t_\tau = 2.30$ °C.

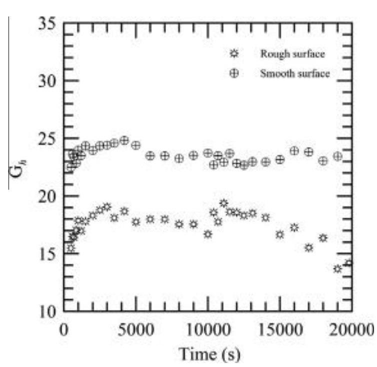

Fig. 10. Time history of defect enthalpy shape factor G_h for the smooth and rough walls.

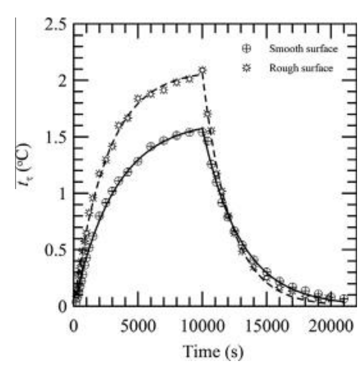

Fig. 12. Friction temperature behavior for the smooth and rough walls.

For the smooth surface case one haves $R_i = -0.0070$, whereas, for the rough surface case, $R_i = -0.0086$. With these values, the logarithmic region of the flow is dynamically neutral.

For the time instants that were considered in this work, the temperature error in origin was always equal to 4.7 mm. The transient response of the temperature error in origin is very short; very quickly ε_T adjusts to its maximum possible value, the height of the protuberances. The determination of ε_T is illustrated in Fig. 11.

The behavior of the friction temperature is shown in Fig. 12 for the smooth surface and rough surface.

The friction temperature was determined directly from the slope of the temperature log-profile. During the heating cycle, the following equation was used for the data reduction

$$T_w - T = \frac{I - Je^{-\sigma t}}{\varkappa_T} \ln(z_T + \varepsilon_T) + B', \tag{41}$$

Table 3
Best-curve fitting parameters for the behavior of t_τ. In the heating cycle: $I = J$; in the cooling cycle: $I = 0$.

Surface	Cycle	σ x10^5	J
Smooth	Heating	31 ± 1	1.65 ± 0.02
Smooth	Cooling	33 ± 1	44.78 ± 1.43
Rough	Heating	39 ± 2	2.09 ± 0.03
Rough	Cooling	46 ± 2	198.93 ± 6.35

where, as justified before, we have considered $\varkappa_T = 0.44$.

In the cooling cycle, $(I - Je^{-\sigma t})$ was replaced simply by $(Je^{-\sigma t})$.

A best-curve fitting to the data in Fig. 12 furnishes Table 3.

The behavior of Stanton number is studied next. For an isothermal flow, the definition of Stanton number results in a mathematical indetermination. In fact,

$$S_t = \frac{u_\tau}{U_\infty}\frac{t_\tau}{T_w - T_\infty}, \tag{42}$$

so that, in isothermal conditions, $t_\tau = 0$, $T_w - T_\infty = 0$ and an indetermination of the type 0/0 is obtained.

However, as soon as heat is applied to the wall, T_w increases above T_∞ resulting in a non-zero value that makes Eq. (42) determined. The standard Reynolds analogy for a smooth wall considers that $(1/2)C_f = S_t$, that is equivalent to say that $u_\tau/U_\infty = t_\tau/(T_w - T_\infty)$.

For a rough surface, corrections need to be proposed in view of the arguments of Owen and Thomson [1]. For fully rough flows, Dipprey and Sabersky [19] suggest

$$S_t = (C_f/2)/[1 + (C_f/2)^{1/2}(5.19R_{e_{K_s}}^{0.2}P_r^{0.44} - 8.48)], \tag{43}$$

where K_s is the equivalent sand roughness, $R_{e_{K_s}}$ denotes $u_\tau K_s/\nu$ and P_r is the Prandtl number.

Kays and Crawford [29] propose

$$S_t = (C_f/2)/[P_{r_t} + (C_f/2)^{1/2}(0.16R_{e_{K_s}}^{0.2}P_r^{0.44})], \tag{44}$$

where P_{r_t} is the turbulent Prandlt number.

Eqs. (43) and (44) were developed for highly compacted sand roughness in pipes. However, since they express the flow behavior in the wall layers, they can be used indistinctly to describe internal or external flows.

In a heating or cooling cycle, if the Stanton number is to be kept constant, t_τ and $T_w - T_\infty$ must vary at the same rate. To investigate this fact, let us promote a best-fit to the time-varying wall temperature profiles shown in Figs. 8a (smooth surface) and 8b (rough surface) according to the curve

$$T_w(t) - T_\infty = M - Ne^{-\Sigma t}. \tag{45}$$

The result is presented in Table 4.

The behavior of the Stanton number can now be evaluated for the limit cases of time tending to zero and to infinity by substituting the fitted curves into Eq. (42), that is,

$$S_t(0) = \lim_{t\to 0}\frac{u_\tau}{U_\infty}\frac{J(1-e^{-\sigma t})}{N(1-e^{-\Sigma t})} = \frac{u_\tau}{U_\infty}\frac{J\sigma}{N\Sigma} \tag{46}$$

and

$$S_t(\infty) = \lim_{t\to\infty}\frac{u_\tau}{U_\infty}\frac{Je^{-\sigma t}}{Ne^{-\Sigma t}} = \frac{u_\tau}{U_\infty}\frac{J}{N}e^{(-\sigma+\Sigma)t}. \tag{47}$$

Therefore, if the Reynolds analogy is to be satisfied at all times, the following relations must hold,

$$\frac{u_\tau}{U_\infty} = \frac{J}{N}, \quad \sigma = \Sigma \tag{48}$$

for both, the heating and the cooling cycles.

Fig. 13 shows the time variation behavior of S_t. The present indication is that for most of the heating cycle S_t remains constant and assumes a value very close to that predicted by Eq. (43). In the cooling cycle, agreement is very good for most of the time, but for very small values of ΔT (=$T_w - T_\infty$) and t_τ where the uncertainties increase.

Table 4
Best-curve fitting parameters for the behavior of $(T_w(t) - T_\infty)$. In the heating cycle: $M = N$; in the cooling cycle: $M = 0$.

Surface	Cycle	Σ x10^5	N
Smooth	Heating	31 ± 1	46.69 ± 0.39
Smooth	Cooling	33 ± 1	1158.69 ± 10.42
Rough	Heating	42 ± 1	46.02 ± 0.72
Rough	Cooling	42 ± 1	3186.44 ± 28.68

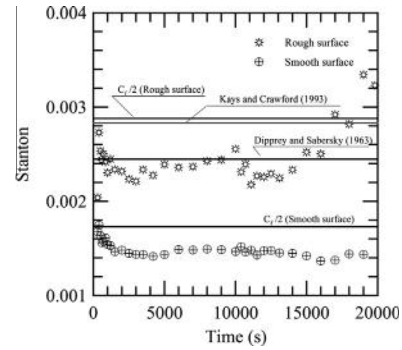

Fig. 13. Stanton number behavior, rough and smooth walls.

Hence, an apparent result from Fig. 13 is that the Reynolds analogy is satisfied for all instants of time. Since the heating and the cooling processes are relatively slowly varying in time, the present problem (at least for some of its properties) can be seen as a sequence of quasi-steady states. That fact allowed us to calculate the time variation of t_τ through the graphical method of Perry and Joubert. However, and despite the t_τ variation, ε_T was observed to remain constant.

Thus, an important result we found here is the marked difference in values for the errors in origin of the velocity and the temperature profiles. In fact, based on the present results and the results of [27], the temperature error in origin seems to be less sensitive to wall geometry alterations, being always much close in value to the height of the protuberances. To situations where the roughness elements are close together (D-type surfaces) this certainly seems to be the case.

For roughness elements which are set close together, we should therefore have $\varepsilon_T > \varepsilon$ ($d_t < d$). The establishment of dead air region between the protuberances normally promotes an inhibition in momentum flux inside the grooves that pushes d to the top of the roughness. The heat transfer process, however, is less affected so that d_t is kept at a lower value. Returning to the fixed geometric relation between d and ε, this is equivalent to say that $\varepsilon_T > \varepsilon$, a result that has been observed here and elsewhere (see, Avelino and Silva Freire [27]).

Finally, we must point out to the reader that if the correct value of ε_T (=4.7 mm) were to be taken mistakenly to be equal to ε (=1.2 mm), the implementation of a computational algorithm based on the application of the law of the wall for the prediction of t_τ would yield errors of the order of 40%.

5. Conclusion

The present work has studied the behavior of the temperature displacement height for transient heating conditions. We have shown that the method of Perry and Joubert [3] works well on these conditions so that it can be successfully used to evaluate the wall heat flux. In particular, we have noticed that, for the problem studied here, the temperature displacement height reaches a constant value in a relatively short time. This constant value is observed to be very different from the velocity displacement height, having instead a value of the order of the height of the roughness protuberances. The consequence is that the wall heat flux can be evaluated directly from the slope of a corrected temperature profile in the fully turbulent region of the flow through Eq. (41).

In fact, all the data reduction took as reference the simple theory here developed. This theory provides indication that under transient condition a logarithmic region can be identified with a constant temperature displacement height but with a time dependent slope.

As far as the Reynolds analogy is concerned, the present indication is that it holds in the transient regime. The results of Table 4 imply that the variations in friction temperature and in wall temperature do present the same decaying rate. Results provided by the correlation of Dipprey and Sabersky [19] furnished a very good prediction of S_t.

Acknowledgements

In the course of the research, JBRL benefited from a CNPq Research Fellowship (Grant No 301172/2010-2) and from further financial support through Grants CNPq 477354/2011-4 and FAPERJ E-26/102.212/2013. APSF is grateful to the Brazilian National Research Council (CNPq) for the award of a Research Fellowship (Grant No 303982/2009-8). The work was financially supported by CNPq through Grant No 477293/2011-5 and by the Rio de Janeiro Research Foundation (FAPERJ) through Grant E-26/102.937/2011.

References

[1] P.R. Owen, W.R. Thomson, Heat transfer across rough surfaces, J. Fluid Mech. 15 (1963) 321–334.
[2] P.S. Jackson, On the displacement height in the logarithmic velocity profile, J. Fluid Mech. 111 (1981) 15–25.
[3] A.E. Perry, P.N. Joubert, Rough-wall boundary layers in adverse pressure gradients, J. Fluid Mech. 17 (1963) 193–211.
[4] A.E. Perry, W.H. Schofield, P.N. Joubert, Rough-wall turbulent boundary layers, J. Fluid Mech. 37 (1969) 383–413.
[5] E.K. Kalinin, G.A. Dreitser, Unsteady convective heat transfer for turbulent flows of gases and liquids in tubes, Int. J. Heat Mass Transfer 28 (1985) 361–369.
[6] J.B.R. Loureiro, F.B.C.C. Sousa, J.L.Z. Zotin, A.P. Silva Freire, The distribution of wall shear stress downstream of a change in roughness, Int. J. Heat Fluid Flow 31 (2010) 785–793.
[7] R.A. Antonia, R. E Luxton, The response of a turbulent boundary layer to a step change in surface roughness. Part 1. Smooth to rough, J. Fluid Mech. 48 (1971) 721–761.
[8] Y. Malhi, The behaviour of the roughness length for the temperature over heterogeneous surfaces, Q. J. R. Meteorol. Soc. 122 (1996) 1095–1125.
[9] J. Sun, Diurnal variations of thermal roughness height over a grassland, Boundary Layer Meteorol. 92 (1999) 407–427.
[10] M.R. Raupach, Anomalies in flux-gradient relationships over forest, Boundary Layer Meteorol 16 (1979) 467–486.
[11] H.A. Einstein, E.-S.A. El-Samni, Hydrodynamic forces on a rough wall, Rev. Mod. Phys. 21 (1949) 520–524.
[12] R.A. Antonia, R.E. Luxton, The response of a turbulent boundary layer to a step change in surface roughness. Part 2. Rough-to-smooth, J. Fluid Mech. 53 (1972) 737–757.
[13] P.J. Mulhearn, A wind-tunnel boundary-layer study of the effects of a surface roughness change: rough to smooth, Boundary Layer Meteorol. 15 (1978) 3–30.
[14] W.P. Elliott, The growth of the atmospheric internal boundary layer, Trans. Am. Geophys. Union 39 (1958) 1048–1054.
[15] H.A. Panofsky, A.A. Townsend, Change of terrain roughness and the wind profile, Q. J. R. Meteor. Soc. 90 (1964) 147–155.
[16] A.A. Townsend, The response of the turbulent boundary layer to abrupt changes in surface conditions, J. Fluid Mech. 22 (1965) 799–822.
[17] A.A. Townsend, The flow in a turbulent boundary layer after a change in surface roughness, J. Fluid Mech. 26 (1966) 255–266.
[18] A. Chan, Atmospheric turbulent boundary layer development due to a change in surface roughness, Int. J. Eng. Sci. 39 (2001) 2001–2014.
[19] D.F. Dipprey, R.H. Sabersky, Heat and momentum transfer in smooth and rough tubes ate various Prandtl numbers, Int. J. Heat Mass Transfer 6 (1963) 329–353.
[20] J.C. Han, L.R. Glicksman, W.M. Rohsenow, An investigation of heat transfer and friction for rib-roughened surfaces, J. Heat Mass Transfer 21 (1978) 1143–1156.
[21] D.S. Johnson, Velocity, temperature and heat transfer measurements in a turbulent boundary layer downstream of a stepwise discontinuity in wall temperature, ASME Trans. J. Appl. Mech. 24 (1957) 2–8.
[22] D.S. Johnson, Velocity and temperature fluctuation measurements in a turbulent boundary layer downstream of a stepwise discontinuity in wall temperature, ASME Trans. J. Appl. Mech. 26 (1959) 325–336.
[23] J.I. Blom, Experimental determination of the turbulent Prandtl number in a developing temperature boundary layer, in: 4th International Heat Transfer Conference, Paris-Versailles, paper FC2.2., vol. II, 1970.
[24] R.A. Antonia, H.Q. Danh, A. Prabhu, Response of a turbulent boundary layer to a step change in surface heat flux, J. Fluid Mech. 80 (1977) 153–177.
[25] H.W. Coleman, R.J. Moffat, W.M. Kays, Momentum and energy transport in the accelerated fully rough turbulent boundary layer, Report No HMT-24, Thermosciences Division, Dept. of Mech. Eng., Stanford University, 1976.
[26] P.M. Ligrani, R.J. Moffat, Thermal boundary layers on a rough surface downstream of steps in wall temperature, Boundary Layer Meteorol. 31 (1985) 127–147.
[27] M.R. Avelino, A.P. Silva Freire, On the displacement in origin for turbulent boundary layers subjected to sudden changes in wall temperature and roughness, Int. J. Heat Mass Transfer 45 (2002) 3145–3153.
[28] B.J. Belnap, J.A. van Rij, P.M. Ligrani, A Reynolds analogy for real component surface roughness, Int. J. Heat Mass Transfer 45 (2002) 3089–3099.
[29] W.M. Kays, M.E. Crawford, Convective Heat and Mass Transfer, third ed., McGraw-Hill, New York, 1993.
[30] H. Schlichting, Boundary Layer Theory, seventh ed., McGraw Hill, New York, 1979.
[31] D.O.A. Cruz, A.P. Silva Freire, On single limits and the asymptotic behaviour of separating turbulent boundary layers, Int. J. Heat Mass Transfer 41 (1998) 2097–2111.
[32] J.B.R. Loureiro, A.P. Silva Freire, Scaling of turbulent separating flows, Int. J. Eng. Sci. 49 (2011) 397–410.
[33] R.L. Simpson, D.G. Whitten, R.J. Moffat, An experimental study of the turbulent Prandtl number of air with injection and suction, Int. J. Heat Mass Transfer 13 (1970) 125–143.
[34] B.F. Blackwell, W.M. Kays, R.J. Moffat, The turbulent boundary layer on a porous plate: an experimental study of the heat transfer behaviour with adverse pressure gradient, Report No HMT-16, Thermosciences Division, Dept. of Mech. Eng., Stanford University,1972.
[35] C.P. Chen, Determination experimentale du nombre de Prandtl turbulent pres d'une parroi lise, Int. J. Heat Mass Transfer 16 (1973) 1849–1862.
[36] I.P. Castro, S. Leonardi, Very-rough-wall channel flows: a DNS study, in: T.B. Nickels (Ed.), IUTAM Symposium on The Physics of Wall-Bounded Turbulent Flows on Rough Walls, 2010.
[37] H. Cheng, P. Hayden, I.P. Castro, A.G. Robins, Flow over cube arrays of different packing density, J. Wind Eng. Ind. Aero. 95 (2007) 715–740.
[38] S.J. Kline, The purpose of uncertainty analysis, J. Fluids Eng. 107 (1985) 153–160.